DOI: https://doi.org/10.24425/amm.2025.155491

D.Q. MINH[©]^{1,2}, N.V.U. NHI[©]^{1,2}, L.T.Q. ANH[©]^{1,2}, K.D.T. KIEN[©]^{1,2*}

USING FLY ASH AS A RAW MATERIAL FOR CERAMIC TILES

Ceramic tiles are among the most commonly used ceramic products. However, the excessive consumption of natural resources poses a significant challenge for this industry. This article presents test results using 0-20 wt.% fly ash as a raw material for producing ceramic tiles fired at 1150°C. Fly ash serves as an alternative to traditional raw materials. The findings demonstrated that a fly ash content of 7.5 wt.% was optimal, resulting in the highest bending strength (45.10 MPa) and favorable values for other parameters, including volumetric density (2.41 g/cm³), actual density (2.48 g/cm³), apparent density (2.43 g/cm³), and water absorption (0.28%), all of which remained within permissible limits. Analysis using X-ray Diffraction and Differential Scanning Calorimetry revealed that the primary mineral constituents of the product are quartz, mullite, fayalite, sillimanite, and albite. Notably, fly ash plays a pivotal role in facilitating mullite formation.

Keywords: Fly ash; ceramic tiles; ceramic; sintering

1. Introduction

Currently, industrial waste is extensively studied for reuse applications in civil engineering, and the reuse of fly ash (FA) from thermal power plants is one of the essential trends [1-5]. Fly ash serves as an alternative source of minerals typically present in the composition of building ceramics. There are chemical composition and fine particle similarities between FA and traditional building ceramics. Both are mixtures of inorganic oxides such as SiO₂, Al₂O₃, Na₂O, Fe₂O₃, CaO, TiO₂, and other minerals [6-9]. Furthermore, it has been concluded that adding FA to a raw mixture enhances the mechanical properties of fired ceramics [10-12].

When reusing FA in the ceramic industry, the main challenge is determining its optimal amount in the initial raw material mixtures concerning the final properties of the ceramic product and the manufacturing process. J.H. Kim et al. [13] used 0-40 wt.% FA addition in the manufacturing process of ceramic wall tiles and observed that the bending strength of ceramic tiles, including 10 wt.% FA, increased to a level comparable to ceramic tiles without FA. The water absorption and porosity of the fired body were slightly altered with increasing fly ash content up to 30 wt.% and decreased with higher FA additions. High calcium

FA (HCFA) was utilized by Rodchom M. et al. as a raw material for ceramic production [14], replacing potash feldspar in amounts of 10-40 (wt.%) at sintering temperatures of 1000-1200°C. The results showed that HCFA promoted the vitrification behavior of ceramic samples. Optimal ceramic properties were achieved by adding HCFA content between 10-30 wt.% and sintering at 1150-1200°C. Based on these favorable mechanical and thermal characteristics, utilizing HCFA as an alternative raw material for manufacturing ceramic tiles is feasible. To maximize the use of FA, Ji R. [14] used alumina-rich FA as the primary raw material for producing porcelain tiles. The rupture modulus of samples containing 60 wt.% FA and 4 (wt.%) quartz reached 51.28 MPa at 1200°C. Moreover, the water absorption, apparent porosity, and linear shrinkage of 0.47 wt.%, 1.1 wt.%, and 13.51 wt.%, respectively, exceed the requirements for porcelain tiles [14].

Most studies have demonstrated physic-mechanical properties such as mechanical strength, volumetric density, water absorption, and shrinkage of the products. Other studies have employed more advanced analytical methods, such as thermogravimetry (TGA), differential thermal analysis (DTA), and thermodilatometry (TDA), combined with X-ray diffractometry (XRD) to provide a more precise explanation of the influence of FA on the firing process of ceramic products [6,8,12].

^{*} Corresponding author: kieudotrungkien@hcmut.edu.vn



HO CHI MINH CITY UNIVERSITY OF TECHNOLOGY (HCMUT), FACULTY OF MATERIALS TECHNOLOGY, 268 LY THUONG KIET STR., WARD 14, DISTRICT 10, HO CHI MINH CITY, VIETNAM

 $^{^2 \}quad \text{VIETNAM NATIONAL UNIVERSITY HO CHI MINH CITY, LINH TRUNG WARD, THU DUC CITY, HO CHI MINH CITY, VIETNAM WARD, THU DUC CITY, HO CHI MINH CITY, WARD, THU DUC CITY, HO CHI MINH CITY, WARD, WARD, THU DUC CITY, HO CHI MINH CITY, WARD, WA$

This paper experimentally investigated the influence of FA (content 0-20 wt.%) on the fundamental properties of ceramic tiles, such as mechanical strength, water absorption, and porosity. The study aimed to determine the optimal FA content that yields the highest flexural strength. To further investigate the sintering changes in this optimal ceramic material sample compared to the FA-free control, thermogravimetric analysis and differential thermal analysis, combined with X-ray diffraction measurements, were performed.

2. Experimental Method

The chemical compositions of FA and samples were determined by X-ray fluorescence (XRF) – equipment used: ARL ADVANT'X – Thermo Brand. The mineral phases in the samples were identified using XRD within a 2θ range of 5° to 70° , with a scan step size of 0.02° . The analysis was conducted on powdered samples using a TOOPIYREAN XRD instrument from the PANalytical brand.

FA was added to the basic ceramic tile mixture consisting of 40 wt.% kaolin, 30 wt.% clay, and 30 wt.% feldspar. The added FA content was 2.5 wt.%, 5 wt.%, 7.5 wt.%, 10 wt.%, 15 wt.%, and 20 wt.% by weight, denoted as F2.5, F5, F7.5, F10, F15, and F20, respectively. F0 serves as the reference sample with 0 wt.% FA.

TABLE 1 delineates the detailed chemical compositions of FA alongside the raw materials employed in the study. By analyzing the data presented in TABLE 1 in conjunction with the standards specified in TCVN 10302:201, it is evident that the FA utilized in these experiments is categorized under class F, characterized by a calcium oxide (CaO) content of less than 5 wt.%. The results from the chemical composition analysis suggest that substituting FA at various proportions does not substantially impact the overall chemical composition of the ceramic matrices. This observation indicates that the intrinsic chemical properties of the ceramic bodies remain largely invariant despite the incorporation of FA at different levels.

The batches were ground in a ball mill, passed through a 63-mesh sieve, and then dried at 110°C for 24 hours in a laboratory dryer. The dry mix powder was moistened to 5-7 wt.% and pressed in a mold of 80×20 mm at a pressure of 4 MPa. The mass of each sample was approximately 25 g \pm 1 g. The pressed

samples were dried at 110°C for 24 hours to prevent deformation during the drying and firing. The samples were fired at 1150°C for 15 minutes in a laboratory furnace.

The physical and mechanical properties of the samples, including bending strength (ASTM C648), water absorption, volumetric density, and actual and apparent density, were determined by ASTM C373 for ceramic tiles.

Compare the bending strength of the samples and identify the sample with the optimal FA ratio based on the criterion of the highest bending strength. Differential Scanning Calorimetry (DSC) analysis was conducted to investigate the changes in thermal properties of the F0 and optimally formulated FA samples across a temperature range of 30°C to 1200°C. The analysis was performed at a heating rate of 10°C/min, using a sample mass of 10 mg, and was carried out with a Differential Scanning Calorimeter (LABSYS EVO). This analysis aims to understand the enhancement of bending strength better.

3. Results and discussions

3.1. The physical and mechanical properties

The experimental results about the bending strength and water absorption of the samples are illustrated in Fig. 1. An analysis of the data highlights the inverse correlation between water absorption and bending strength. Specifically, as water absorption increases, the bending strength correspondingly decreases. This trend is evident in the sample designated as F7.5, which has emerged as the optimal formulation among the tested samples. F7.5 achieved a remarkable peak bending strength of 45.10 MPa, showcasing its superior mechanical properties. Additionally, the F7.5 sample demonstrated a low water absorption rate of 0.28 wt.%. This minimal water uptake reinforces the sample's high bending strength and underscores its robustness and durability in varying environmental conditions. Such properties are especially advantageous in fields like construction, where materials are routinely exposed to moisture. The performance metrics of the F7.5 sample suggest its potential for broad usage in various high-stress and high-performance environments.

Additionally, Fig. 2 provides an overview of the volumetric, actual, and apparent density for a range of samples. According to

The Chemical compositions of FA and samples (wt.%)

Chemical compositions (wt.% oxide) Denote of Sample TiO₂ L.O.I SiO₂ Al₂O₃ Fe₂O₃ K₂O CaO Na₂O MgO other F0 57.01 21.07 6.26 1.76 2.80 0.32 1.79 5.79 3.63 0.12 21.16 1.75 2.81 F2.5 56.92 6.25 0.403.55 0.13 1.75 5.83 F5 56.83 21.25 6.24 1.73 2.81 0.483.46 1.71 5.87 0.14 F7.5 56.73 21.34 6.22 1.71 2.82 0.56 3.38 0.16 1.67 5.91 F10 56.64 21.44 6.21 1.70 2.82 0.643.29 0.17 5.95 1.63 F15 56.46 21.62 6.18 1.67 2.83 0.803.12 0.20 6.03 1.55 F20 0.96 2.95 56.27 21.80 6.15 1.63 2.84 0.221.47 6.11 24.72 1.12 2.99 3.50 0.24 0.197.40 FΑ 53.33 5.71 0.65

(*) Loss on ignition

TABLE 1

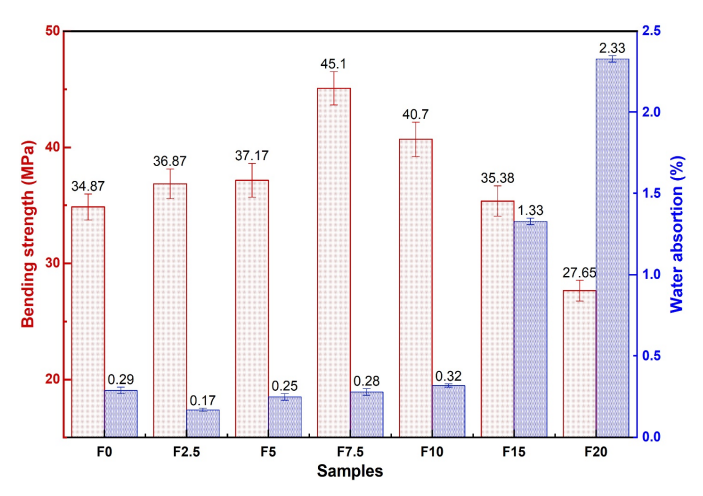


Fig. 1. The bending strength and water absorption of the samples

the data analyzed in compliance with the EN 177 specifications, all samples meet the BIIa classification criteria. This classification signifies that ceramic materials demonstrate practical and reliable properties, ensuring their suitability and robustness for real-world applications. The compliance with the BIIa classification indicates that these ceramic materials are engineered to perform efficiently under various conditions, showcasing their durability and reliability.

Sample F 7.5 had the highest bending strength, but its water absorption, volumetric density, actual density, and apparent density were not the lowest. Thus, the quality of the bond formed in the the sample played a decisive role in this case. The XRD analysis results below will show us the compounds formed in the test samples.

3.2. The results of XRD analysis

The XRD patterns of the samples are shown in Fig. 3. The XRD analysis indicates the mineralogy transformations occur-

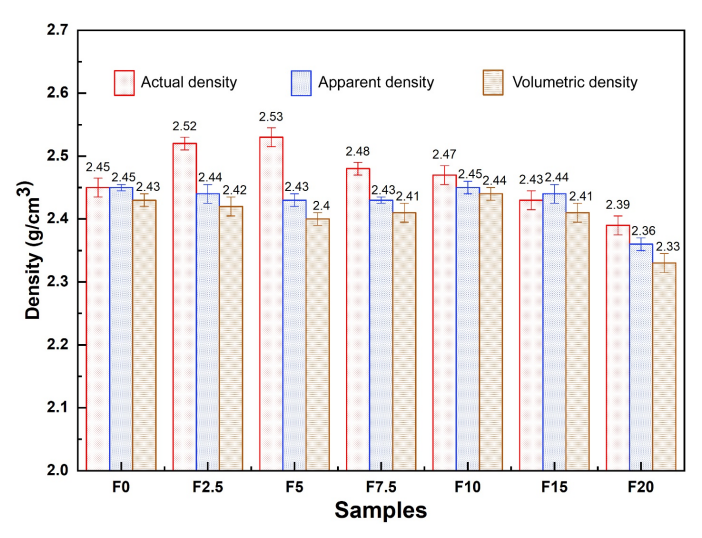


Fig. 2. The volumetric density, actual and apparent density of the samples

ring in the ceramic green bodies after firing at 1150°C. The prefired FA sample was initially characterized by the presence of quartz (observed at 20.84°, 26.63°, and 50.12°), mullite (detected at 16.48°, 42.85°, and 19.72°), and hematite (seen at 33.17°, 35.65°, and 40.88°), as reported in previous studies [15-17]. In contrast, the raw, unburnt sample labeled F0 contained quartz, as well as albite (identified at 22.01° and 28.26°) and kaolinite (seen at 12.42° and 25.52°) minerals [15,18-20].

Upon subjecting the samples to a firing temperature of 1150°C, significant mineralogical changes were observed. The kaolinite and albite minerals in all samples, with varying FA content from 0 wt.% to 20 wt.%, transformed. These minerals were converted into mullite, quartz, sillimanite (identified at 35.30° and 40.91°), and fayalite (detected at 33.99°, 19.87°, and 39.02°). The synthesis of mullite through the transformation of clay minerals and fly ash has been extensively documented in prior research [15,16,21,22]. The transformation process can be clarified using chemical Eqs. (1) to (4). This transformation

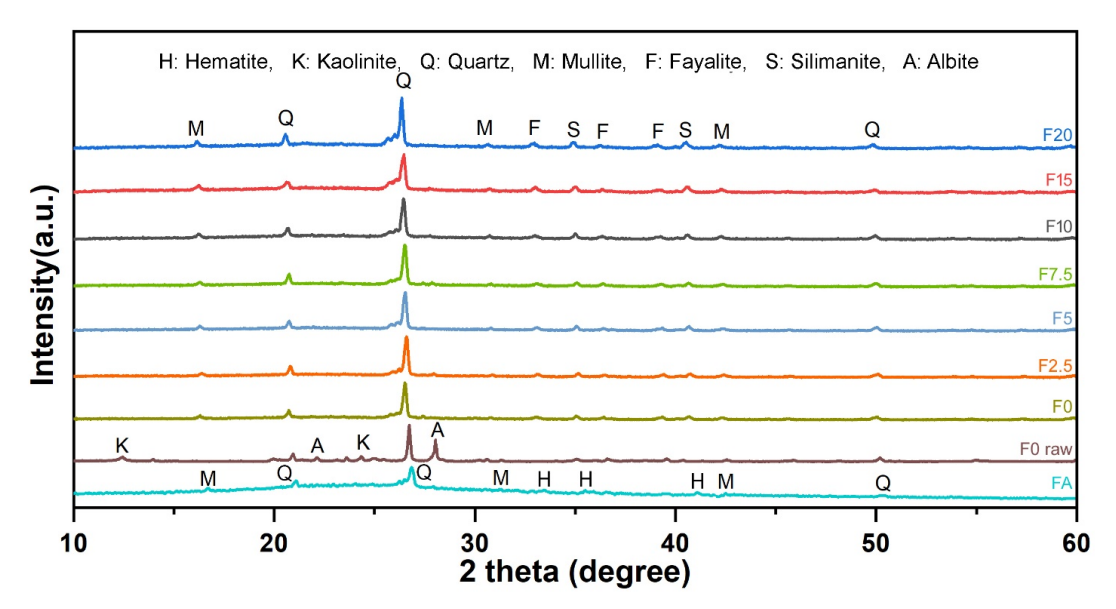


Fig. 3. The XRD patterns of samples

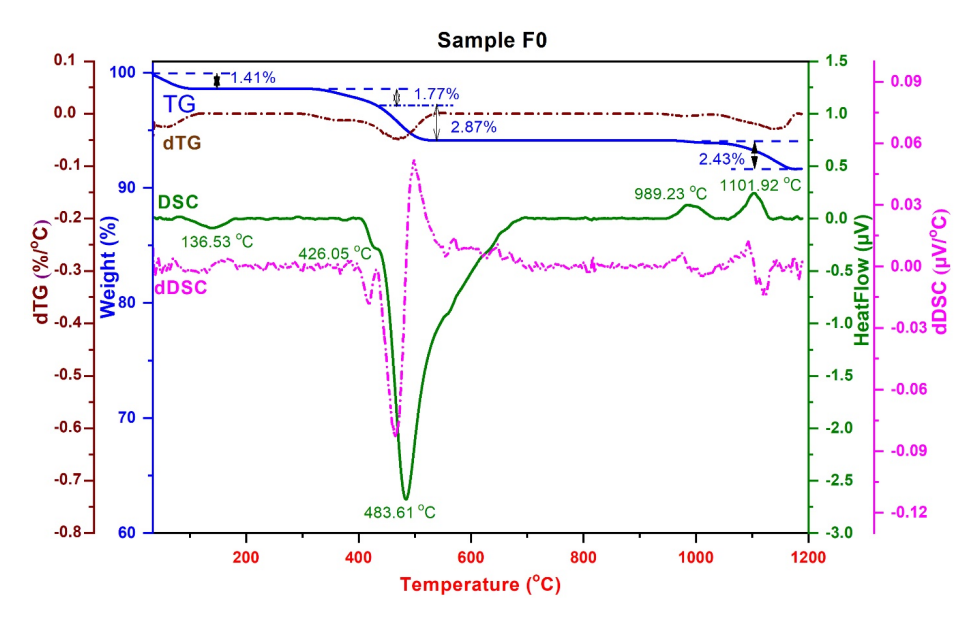
indicates a substantial alteration in the crystalline structure, contributing to developing the desired ceramic properties through the high-temperature firing process.

$$\begin{split} 2(\text{Al}_2\text{O}_3.2\text{SiO}_2) &\overset{900-1000^\circ\text{C}}{\to} 2\text{Al}_2\text{O}_3.3\text{SiO}_2 + \text{SiO}_2 \\ & \qquad \qquad (2:3 \text{ spinel}) \end{split} \tag{1} \\ 2\text{Al}_2\text{O}_3.3\text{SiO}_2 &\overset{900-1000^\circ\text{C}}{\to} 2(\text{Al}_2\text{O}_3.\text{SiO}_2) + \text{SiO}_2 \\ & \qquad \qquad (1:1 \text{ silimanite}) \end{aligned} \tag{2} \\ 3(\text{Al}_2\text{O}_3.\text{SiO}_2) &\overset{1150^\circ\text{C}}{\to} 3\text{Al}_2\text{O}_3.2\text{SiO}_2 + \text{SiO}_2 \\ & \qquad \qquad (3:2 \text{ mullite}) \end{aligned} \tag{3} \\ \text{Fe}_2\text{O}_3 + \text{SiO}_2 &\overset{1000-1150^\circ\text{C}}{\to} \text{Fe}_2\text{O}_3. \text{SiO}_2 \end{split}$$

(Fayalite)

3.3. The results of DSC analysis

Fig. 4. and Fig. 5. display DSC, DDSC, TG, and DTG curves for the samples F0 and F7.5. The thermal effect observed in the DSC curves occurs at approximately 77.35°C for the F0 sample and 74.58°C for the F7.5 sample, indicating the release of physically bound water from the raw materials in both samples. Corresponding to these thermal effects, the TG curves show mass losses of 1.41 wt.% for F0 and 0.83 wt.% for F7.5. The second set of thermal effects is minor, occurring around 426.05°C and 409.16°C in the DSC curves of the F0 and F7.5 samples, respectively. These thermal effects correlate with mass losses of 1.77 wt.% for F0 and 0.84 wt.% for F7.5, as indicated by the TG curves. These phenomena can be attributed to the raw samples' pyrolysis of residual organic materials and carbon. Subsequent thermal effects are observed at approximately 483.61°C and 490.92°C,



(4)

Fig. 4. The DSC curves of F0 samples

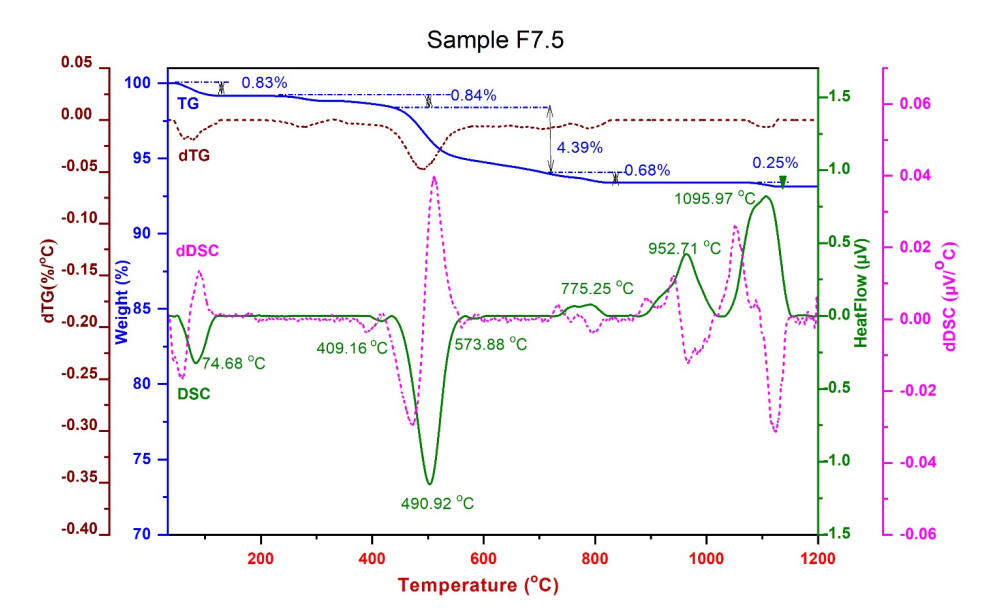


Fig. 5. The DSC curves of F7.5 samples

corresponding to mass losses of 2.87 wt.% for F0 and 4.39 wt.% for F7.5, respectively. These effects are indicative of the dehydration reactions occurring in clay minerals. Additionally, the allotropic transformation of α -quartz to β -quartz is recorded at 574.25°C for the F0 sample and 573.88°C for the F7.5 sample.

The exothermic effect observed at 775.25°C appears exclusively in the DSC curve of sample F7.5, corresponding to the transformation of calcite present in the FA. As the F0 sample does not contain CaO, no similar effect is observed in its DSC curve. Initially, the decomposition of calcite (CaCO₃) to CaO is indicated by a mass loss in the TG curve [23,24]. Subsequently, CaO reacts with silicon dioxide (SiO₂) to form calcium silicates, resulting in an exothermic effect in the DSC curve [25].

The exothermic effect observed in both DSC curves within the temperature range of 900-1200°C corresponds to the formation of the mineral's spinel and mullite, as described by chemical reactions 1-4 [25].

It can be inferred that the quantity of mullite crystallized is proportional to the area of the effect region in the DSC curve. The area of the mullite crystallization region in the F7.5 sample, at 478.96 J/g, is significantly larger than that of the F0 sample, at 144.04 J/g. Therefore, it can be concluded that including fly ash (FA) facilitates mullite formation during the firing of these ceramic tiles.

4. Conclusions

The impact of varying fly ash content, ranging from 0 to 20 wt.%, on the properties of ceramic tiles was thoroughly evaluated. The research findings indicate that the incorporation of FA at a concentration of 7.5 wt.% yields the highest flexural strength among the tested samples. This enhancement in mechanical performance is notable, while other key properties, such as volumetric density and water absorption, remain within the acceptable limits established for ceramic tiles. XRD and DSC analyses further substantiate these findings. The results from the XRD analysis demonstrate an increase in mullite content, a valuable phase known for its high thermal stability and mechanical strength, which is a beneficial outcome of using FA. The DSC data corroborate this observation by indicating significant exothermic effects associated with mullite formation. The ability of fly ash to enhance mullite formation underscores its potential as a functional material in ceramic production. The data suggests that fly ash can effectively contribute to producing high-performance ceramic tiles when used at an appropriate concentration. Therefore, it can be concluded that fly ash, a by-product from thermal power plants, is a viable and advantageous raw material for manufacturing ceramic tiles, offering both performance benefits and environmental sustainability.

Acknowledgments

We acknowledge Ho Chi Minh City University of Technology (HCMUT), VNU-HCM for supporting this study.

REFERENCES

- [1] E. Fidanchevski, B. Angjusheva, V. Jovanov, P. Murtanovski, L. Vladiceska, N.S. Aluloska, J.K. Nikolic, A. Ipavec, K. Ster, M. Mrak, S. Dolenec, Technical and radiological characterization of fly ash and bottom ash from thermal power plant. J. Radioanal. Nucl. Chem. 330, 685-694 (2021).
- [2] G. Khambra, P. Shukla, Novel machine learning applications on fly ash based concrete: an overview. Mater. Today: Proceedings, 8, 3411-3417 (2023).
- [3] H.H.T. Nguyen, H.T. Nguyen, S.F. Ahmed, N. Rajamohan, M. Yusuf, A. Sharma, P. Arunkumar, B. Deepanraj, H.T. Tran, A.A. Gheethi, D.V.N. Vo, Emerging waste-to wealth applications of fly ash for environmental remediation: A review. Environ. Res. 227, 115800 (2023).
- [4] L. Sawunyama, O.C. Olatunde, O.A. Oyewo, M.F. Bopape, D.C. Onwudiwe, Application of coal fly ash based ceramic membranes in wastewater treatment: A sustainable alternative to commercial materials. Heliyon 10, e24344 (2024)
- [5] J.C. Ge, S.K. Yoon, N.J. Choi, Application of fly ash as an adsorbent for removal of air and water pollutants. Appl. Sci. **8**, 1116 (2018).
- [6] Y.K. Cho, S.H. Jung, Y.C. Choi, Effects of chemical composition of fly ash on compressive strength of fly ash cement mortar. Constr. Build. Mater. 204, 255-264 (2019).
- [7] R.E. Bickelhaupt, Surface resistivity and the chemical composition of fly ash. J. Air Pollut. Control Assoc. 25 (2), 148-152 (1975).
- [8] T. Okada, H. Tomikawa, Effects of chemical composition of fly ash on efficiency of metal separation in ash-melting of municipal solid waste. Waste Manage. 33 (3), 605-614 (2013).
- [9] L. Du, E. Lukefahr, A. Naranjo, Texas Department of Transportation fly ash database and the development of chemical composition–based fly ash alkali-silica reaction durability index. J. Mater. Civ. Eng. 25 (1), 70-77 (2013).
- [10] I. Queralt, X. Querol, A. López-Soler, F. Plana, Use of coal fly ash for ceramics: a case study for a large Spanish power station. Fuel **76** (8), 787-791 (1997).
- [11] Z. Haiying, Z. Youcai, Q. Jingyu, Study on use of MSWI fly ash in ceramic tile. J. Hazard. Mater. **141** (1), 106-114 (2007).
- [12] C. Ferreira, A. Ribeiro, L. Ottosen, Possible applications for municipal solid waste fly ash. J. Hazard. Mater. 96 (2-3), 201-216 (2003).
- [13] J.H. Kim, W.S. Cho, K.T. Hwang, K.S. Han, Influence of fly ash addition on properties of ceramic wall tiles. Korean J. Mater. Res. **27** (2), 76-81 (2017).
- [14] M. Rodchom, P. Wimuktiwan, K. Soongprasit, D. Atong, S. Vichaphund, Preparation and characterization of ceramic materials with low thermal conductivity and high strength using high-calcium fly ash. Int. J. Miner. Metall. Mater. 29, 1635-1645 (2022).
- [15] N. Marinoni, M.A. Broekmans, Microstructure of selected aggregate quartz by XRD, and a critical review of the crystallinity index. Cem. Concr. Res. 54, 215-225 (2013).
- [16] H. Schneider, J. Schreuer, B. Hildmann, Structure and properties of mullite a review. J. Eur. Ceram. Society **28** (2), 329-344 (2008).

- [17] G. Schimanke, M. Martin, In situ XRD study of the phase transition of nanocrystalline maghemite (γ -Fe₂O₃) to hematite (α -Fe₂O₃). Solid State Ion. **136**, 1235-1240 (2000).
- [18] S. Gomes, M. François, Characterization of mullite in silicoaluminous fly ash by XRD, TEM, and 29Si MAS NMR. Cem. Concr. Res. **30** (2), 175-181 (2000).
- [19] D. Feng, J.L. Provis, J.S.V. Deventer, Thermal activation of albite for the synthesis of one-part mix geopolymers. J. Am. Ceram. Soc. **95** (2), 565-572 (2012).
- [20] P. Aparicio, E. Galán, R. Ferrell, A new kaolinite order index based on XRD profile fitting. Clay Miner. **41** (4), 811-817 (2006).
- [21] Y. Igami, S. Ohi, A. Miyake, Sillimanite-mullite transformation observed in synchrotron X-ray diffraction experiments. J. Am. Ceram. Soc. **100** (10), 928-4937 (2017).

- [22] J.S. Zhang, Y. Hu, H. Shelton, J. Kung, P. Dera, Single-crystal X-ray diffraction study of Fe2SiO4 fayalite up to 31 GPa. Phys. Chem. Miner. **44**, 171-179 (2017).
- [23] J. Kováč, A. Trník, I. Medveď, I. Štubňa, L. Vozár, Influence of fly ash added to a ceramic body on its thermophysical properties. Therm. Sci. **20** (2), 603-612 (2016).
- [24] R. Frost, M. Hales, W. Martens, Thermogravimetric analysis of selected group (II) carbonateminerals – Implication for the geosequestration of greenhouse gases. J. Therm. Anal. Calorim. 95, 999-1005 (2009).
- [25] G. Brindley, M. Nakahira, A new concept of the transformation sequence of kaolinite to mullite. Nature **181**, 1333-1334 (1958).